Axial Length Measurement

11

David L. Cooke

Introduction

Optical biometry has markedly improved postoperative predictions after cataract surgery. Prior to this time, ultrasound (US) was the standard. The IOLMaster (Carl Zeiss, Jena, Germany) was markedly less user-dependent, and its axial length (AL) measurements were shown to be more repeatable than those by US biometry; it became the gold standard shortly after its release in 1999.

For nearly 20 years, there has been only one way to optically measure the AL—the way Haigis set up in late 1990s and published in 2000. It is used in the IOLMaster (version 500 and earlier), and most competitors have tuned their machine to that method. It has been unclear what to label this AL. It has been called "Axial Length Measurements Based on Single Refractive Index" [1], "Composite method for acquiring optical axial length" [2], "Axial Length Using a Single Group Refractive Index" [3], and "Displayed AL" [3]. There are some problems with each of these labels. In this chapter, it will be called "Traditional AL."

Recently, another method has arisen, where the segment lengths are added together and a theoretical retinal thickness (fudge factor) is subtracted from all values until the average AL for the dataset is equal to the average IOLMaster AL. It has correctly been called by at least all these labels, "Segmented AL," "Segmental AL," "Segment-wise AL," "Axial Length Measurements Based on Multiple Refractive Indices," "Segmental method for acquiring optical axial length," and "Axial Length Using different Refractive Indices for Each Ocular Segment." In this chapter, it will be called sum-of-segments AL.

The goal of this chapter is to explain and explore these two AL methods. Topics will be presented in this order, with these headings: basic science, definitions of commonly used terms, history, ocular segments, and areas for potential improvement.

Basic Science

Axial Length Measurements

Since the geometric length of the eye or its segments cannot be measured directly (such as using a ruler or caliper), technologies had to be developed to measure them *indirectly*. Two of them which provide adequate resolution for ophthalmic purposes are US and optical biometry.

D. L. Cooke (✉)
Department of Neurology and Ophthalmology, Michigan State University, College of Osteopathic Medicine, East Lansing, MI, USA

Great Lakes Eye Care, St. Joseph, Michigan, USA

J. Aramberri et al. (eds.), *Intraocular Lens Calculations*, Essentials in Ophthalmology,
https://doi.org/10.1007/978-3-031-50666-6_11

Ultrasound (US) Biometry

US biometry measures the time (T) that sound takes to reflect off the interfaces in the eye. These times are converted to geometrical lengths by multiplying the time by the sound velocities V.

$$\text{Length} = T_{\text{measured}} * V_{\text{Media}} \tag{11.1}$$

Early US machines only measured reliable signals from the retina internal limiting membrane (ILM). Later, high-precision immersion US systems, like those used today, detected signals from the ocular segments as well. Besides providing the individual segmental lengths (aqueous, lens, vitreous), these systems provided the initial sum-of-segments axial length measurements of the eye. Widely used sound velocities are $V_{\text{aqueous}} = 1532$ m/s, $V_{\text{lens}} = 1641$ m/s, and $V_{\text{vitreous}} = 1532$ m/s.

Carefully performed, segmental immersion ultrasound measurements provide the most accurate US sum-of-segments ALs. There are some drawbacks compared to optical biometry, however. Because US reflects off the ILM, retinal pathologies such as an epiretinal membrane, may adversely affect US ALs. In addition, its resolution and reproducibility are less than those of optical biometry.

Optical Biometry (Interferometry)

All optical biometers and OCTs (Optical Coherence Tomography) are interferometers. The original, time-domain biometers work in this fashion (see Fig. 11.1): a beam of light is emitted from the machine toward the eye, passing through a beam splitter. Beam 1 travels to the eye, and beam 2 travels through air to a moveable mirror. After reflections, these beams travel to a photosensor which detects the intensity of light formed by the constructive and destructive interference of the two beams.

Reflections of beam 1 occur where there are sharp changes in refractive index such as at media boundaries. Spikes from constructive interference occur when the optical time for beam 1 to travel from the light source to the eye and back to the photodetector is identical to the optical time for beam 2 to travel from the light source to the beam splitter, to the moveable mirror, and back to the photodetector.

The mirror may move either backward or forward. For this example, it will move backward. As it does, an initial photodetector spike is generated due to beam 1 reflection from the anterior cornea. This is typically the reference point for the rest of the measurements. As the mirror moves further, the next spike occurs at the posterior corneal surface. The distance moved by the mirror between the first and the second spikes is the "air distance" or "optical path length" (OPL) of the cornea. The distance the mirror moves between the second and third spikes is the OPL of the aqueous and so on through the eye.

If we knew the speed of light through the cornea (mm/s), and we knew the time (s) it took to travel through the cornea, we could multiply the speed of light by that time to get the true geomet-

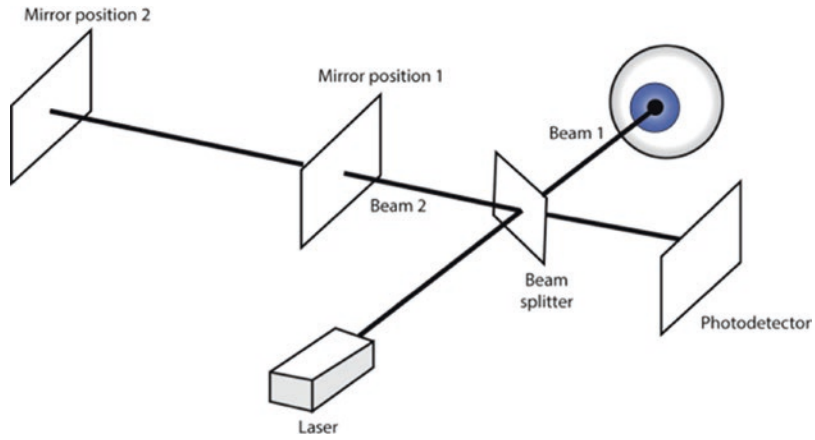

Fig. 11.1 Interferometer

ric thickness of the cornea in mm. Unfortunately, we cannot directly measure the speed of light in the cornea. However, because the refractive index (RI) is the ratio of the speed of light in the cornea to the speed of light in air, we can set up the following ratios:

$$\frac{\text{Speed of light in air}}{\text{Speed of light in cornea}} = \text{RI} = \frac{\text{Air length of cornea}\left(\text{OPL}\right)}{\text{Geometric corneal length}} \tag{11.2}$$

Rearranging this equation, we can determine the geometric length of the cornea

$$\text{Geometric length} = \frac{\text{OPL}}{\text{RI}} \tag{11.3}$$

where OPL is the optical path of the cornea and RI is the refractive index of the cornea.

Newer instruments use more efficient methods of interferometry than time-domain interferometry, such as swept-source interferometry. The concepts of air distance, optical path length, and refractive indices all still apply to every optical biometer as well as to every OCT machine.

An optical biometer produces a picture that is very similar to an ultrasound A-scan (Fig. 11.2). The OCT lines up several optical "A-scans" to create a two-dimensional image in the same way an ultrasound B-scan lines up several A-scans to create a two-dimensional image. The OCT is an "optical B-scan" while a simple optical biometer is an "optical A-scan."

Refractive Indices (RIs)

Refractive indices are typically measured with a refractometer that is temperature-controlled between 20 and 25 °C because temperature has a large effect on refractive index. It is customary for a single wavelength to be used, such as the sodium D line at 589 nm. Refractive indices in literature typically refer to this D line. The refractive index of a single wavelength is called a phase RI. A group RI results when more than one wavelength is used, as is the case with partial or low-coherent light.

Scaling Formulas

A prism-induced "rainbow" is a good demonstration of the speed of light varying by wavelength. If all wavelengths traveled at the same speed, white light would exit a prism the same way it entered, as white light. Obviously this isn't the case. The shorter, violet wavelengths are bent most. That is the same as saying the RI of violet waves is higher than for longer red waves.

The rule to remember is that as a light wavelength changes, one must use a different refractive index for the same substance. An example might be the aqueous. Gullstrand found a phase refractive index of 1.336. It is a bit unclear whether this was at green light (555 nm) or yel-

Fig. 11.2 Typical "A-scan" produced by an optical biometer. The first spike is the reflection produced by the air–corneal interface of the anterior cornea. The first "×" is above the spike produced at the posterior cornea. The second "×" is above the spike of the anterior capsule of the crystalline lens. The third "×" is above the spike of posterior capsule; the fourth "×" is above the junction of the anterior retina and the vitreous. This spike is not visible in some eyes. The final "×" is above the spike of the retinal pigment epithelium

low light (593 nm). However, it is clear that for a light wave of 1050 nm—the light wave of the ARGOS biometer (Movu, Santa Clara, California) [4]—the RI should be a different value than 1.336, the value ARGOS uses.

Because the change in RI by wavelength is not linear, scaling formulas are necessary. These formulas attempt to predict what the RI of a substance (e.g., the cornea) will be at different wavelengths.

The key points from the basic science section

- All OCTs and optical biometers measure an "air distance" which must be divided by a group refractive index to determine the actual length of an ocular segment, such as the cornea.
- Gullstrand RIs apply to green or yellow light, but likely not to the invisible wavelength used in optical biometers.
- Because the actual group RIs for the measuring wavelengths of biometers at body temperatures aren't known, we don't know the actual thicknesses of the ocular segments. Instead, the axial length was calibrated to ultrasound AL of the eye (discussed further in the "History" section).
- Though current measurements may not be physiologically accurate, both US AL and optical AL could be physically correct if either correct sound velocities (V) or group refractive indices (RIs) were known.

Definitions of Commonly Used Terms.

Coherence

The term "coherence" is used in the label of many ocular machines: OCT (optical coherence tomography), OLCR (optical low-coherence reflectometry), OLCI (optical low-coherence interferometry), and PCI (partial coherence interferometry). The ARGOS has been called a "large-coherence length" swept-source OCT.

The difference between coherent and non-coherent light is in the capability of generating interference. Generally speaking, if incoherent light arrives from two sources, its intensity just adds up from the two sources and you see the illuminated spot brighter. For example, by shining two flashlights at the same spot at night, you get twice the intensity.

From our interferometry example, beams 1 and 2 both go to separate mirrors and instead of having the beams converge on a photosensor, they project onto a screen. When both beams travel the same distance in air (OPL), the optical path difference (OPD) between the two paths is zero.

For each tiny part of the final image, the two waves either amplify or weaken each other, depending on the OPD between the two beams at that exact point. If the OPD = 0, constructive interference happens and the intensity increases to 4 times that of a single beam. If the OPD = half a wavelength, then the peak of one wave meets the trough from the other wave, and they cancel each other out leading to an intensity of zero at that spot. This often causes adjacent bright and dark lines referred to as interference fringes (see Fig. 11.3). The pattern of lines on the screen looks like fingerprint lines. The main difference between coherent and incoherent light is that the former interferes causing fringes while the latter just makes the spot brighter.

If a beam of white light is used in our interference example, you will see fringes when the OPD between the two paths is zero. When OPD is increased very slightly, the fringes "wash out" and you just see a spot of light. For a Helium–Neon (HeNe) laser, you can move one mirror by 25 m and still get interference fringes. Coherence

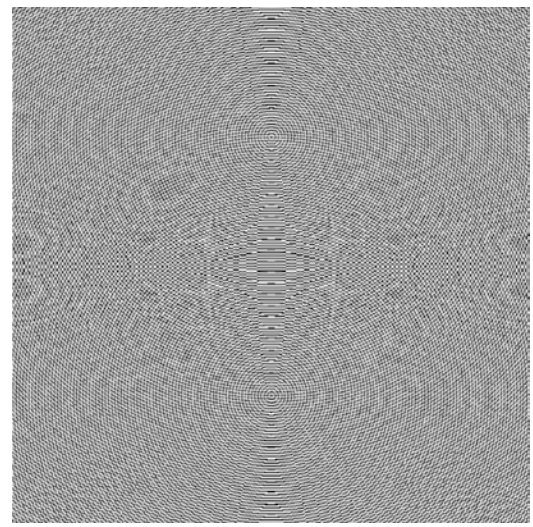

Fig. 11.3 Interference fringe

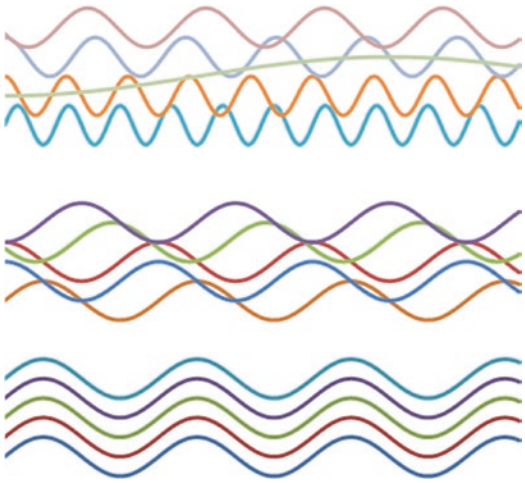

Fig. 11.4 Coherence diagram. Waves align for highly coherent light (bottom row); they partially align for partial coherence light (middle row). Incoherent waves do not align (top row)

length is the OPD between the two beams over which you still get interference fringes. In other words, the coherence length is the maximum OPD between the two paths of an interferometer over which the light wave maintains a harmonic shape such that you can still see interference fringes (before the fringes wash out).

White light has a very short coherence length of a few nm. Low coherence length is approximately 160 μm [5], and large coherence length is in the range of 15–30 mm [6]. "Partial coherence," "low coherence," and "short coherence length" are equivalent terms (Fig. 11.4). Reflectometer is another name for interferometer (in an ophthalmology setting).

Group RI

Group RI and *phase RI* are often discussed together because they are related. The refractive index of a single wavelength, such as a HeNe laser, is called a *phase RI*. Biometers use laser diodes or super-luminescent diodes which emit a bandwidth centered about a single wavelength. The bandwidth reduces the coherence length. This group of wavelengths is treated as if it were one wavelength. It is called a *group RI*, and it has a slightly different RI than the *phase RI*.

History

Haigis calibrated optical biometry to segmental immersion US AL measurements. He calculated a weighted-average of the segment group refractive indices (RIs). Note that he didn't use segment phase RIs, and note that the weighted average RI is not called a group RI.

In the English literature, he measured only 98 eyes with both immersion US biometry and optical biometry optical path lengths (OPLs) [7]. However, he actually measured more than 600 eyes [8], and he later confirmed this with 320 eyes, obtaining 5 measurements for each eye [9]; he then correlated optical biometry OPL with immersion sum-of-segments US AL. He couldn't calculate optical biometry sum-of-segments AL because the IOLMaster could only measure two spikes: one at the anterior cornea and one at the retinal pigment epithelium (RPE).

He initially used a weighted-average group refractive index RI ("composite RI") approximated from the Gullstrand eye (1.3549). However, a regression formula worked better than using the average RI. He kept 1.3549 in the formula, and this decision has caused some confusion. When a regression includes a formula, the regression often undoes it, creating a new formula instead. Haigis showed this in a German-language article [10]. Haigis stated that the original formula (containing the composite RI of 1.3549) used in the IOLMaster algorithm:

$$AL_{GBS} = \left(OPL_{IOLMaster} / 1.3549 - 1.3033\right) / 0.9571 \tag{11.4}$$

was identical to this new formula, which he labeled "calibration function":

$$AL_{Zeiss} = 0.7711 \times OPL_{IOLMaster} - 1.3617 \tag{11.5}$$

AL_{GBS} was the measured segmental immersion US AL. Haigis replaced this with AL_{Zeiss} which is the algorithm used in the IOLMaster (version 500 and earlier). Haigis emphasized, "Consequently, the calibration function (Eq. 11.5) also contains no group refractive indices as a variable." Simply-put, he had the OPL and found a regression which converted that OPL to an ultrasound-equivalent AL. When he regressed to US, it negated the average group RI of 1.3549. Any RI could have been included in that original formula, and the regression coefficients would have changed accordingly, ending up with Eq. (11.5).

Shortly after the IOLMaster was introduced, debate arose as to whether Haigis had properly calibrated it. At least two groups which use ray-tracing [11, 12] used a different calibration algorithm. Fam [13] and later Wang [14] adjusted the biometric parameters for eyes of certain ALs, to compensate for observed refractive errors.

Haigis's calibrated AL (Eqs. 11.4 or 11.5) has become the traditional AL to which other biometers have been calibrated [10]. It is important to note that this distance is not the physiological AL, from the anterior cornea to the RPE (where the photoreceptors lie), but rather from the anterior cornea to the internal limiting membrane of the retina.

Lenstar

When Haag-Streit initially developed the Lenstar, its plan was to use sum-of-segments AL instead of traditional AL. However, in order to release the Lenstar with the FDA's 510K-approval [15], the Lenstar had to be made substantially equivalent to the IOLMaster. Because of this, Haag-Streit disabled the sum-of-segments capability. It would only be available as a research option.

Sum-of-Segments AL

Sum-of-segments AL is quite different from traditional AL at the extremes. Compared to sum-of-segments AL, traditional AL is shorter for short eyes and longer for long eyes. Figure 11.5 illustrates the difference between these two methods of calculating optical AL. Trend lines are plotted instead of the actual data from the 1442 eyes which were used to develop these trend lines. Figure 11.5a is a Bland-Altman plot which shows that sum-of-segments AL is the same length as traditional AL in the normal AL range of 24 mm, but not at the extremes.

The effect of sum-of-segments AL on prediction errors is illustrated in Fig. 11.5b. Prediction errors are about the same for both methods of calculating AL, when ALs are in the typical range of approximately 24 mm. At extreme ALs, sum-of-segments AL (dashed line in Fig. 11.5b) gave a

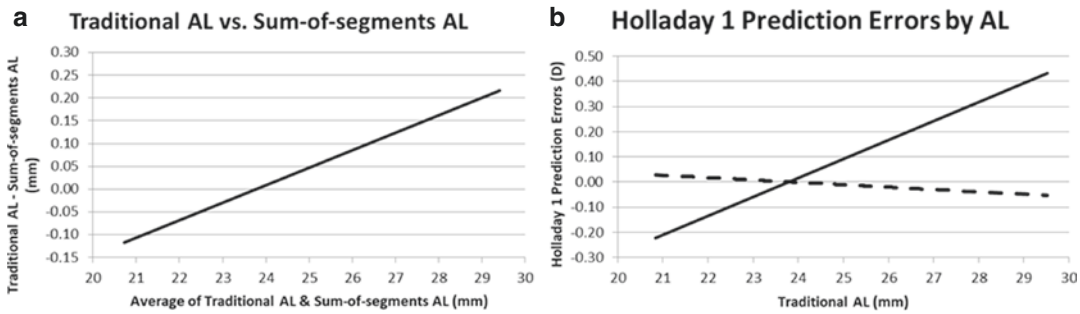

Fig. 11.5 (**a**) (Left) Bland-Altman graph of traditional AL vs. sum-of-segments AL, using the trend line of 1442 ALs measured with Lenstar. Axial length was calculated by two methods: traditional AL and sum-of-segments AL (modified from Cooke and Cooke [16]). (**b**) (Right) shows the trend lines of 1442 Holladay 1 prediction errors by traditional AL and sum-of-segments AL (modified from Cooke and Cooke [16]). The solid line represents the prediction error when using traditional AL. Sum-of-segments AL was used in calculating the dashed line. All other formula inputs were identical, including lens constants

notable improvement over using Holladay 1 with traditional AL (solid line) and it nearly optimized the Holladay 1 prediction error trend line.

The dashed line in Fig. 11.5b illustrates the findings of at least two studies [3, 16], which have shown that original vergence formulas (such as Holladay 1) are improved when sum-of-segments AL is used instead of traditional AL. The Olsen formula is known to have an internal AL recalibration. As expected, it was shown to be worse with sum-of-segments AL in both studies. Presumably, newer formulas have internal AL adjustments for long and short eyes such that they would perform worse when using sum-of-segments AL than when using traditional AL.

For most biometers, segment OPLs are only available in a research mode, if they are available at all. Because sum-of-segments AL requires these segment OPLs, we developed a way to closely approximate sum-of-segments AL using CMAL (Cooke-modified AL). CMAL does not require OPLs, but rather, uses displayed biometer values:

$$\text{CMAL} = 1.23853 + 0.95855 \times \text{traditional AL} - 0.05467 \times \text{lens thickness} \tag{11.6}$$

where all measurements are in millimeters. CMAL seems to work well on the Lenstar, but it still needs to be validated with other machines. Theoretically, it should work for all biometers, assuming that the displayed lens thickness (LT) and AL are equivalent between that biometer and the Lenstar machine. However, this does not mean CMAL represents the true axial length because it is based on the Lenstar group refractive indices. Also, there is not necessarily industry-wide agreement as to where on a spike to place the cursors. Referring to Fig. 11.2, the second "×" is above the spike of the anterior capsule of the crystalline lens. Perhaps this is incorrect. Perhaps it should be placed at the initiation (i.e., bottom) of the spike.

Not all segments are equivalent between biometers. For example, the ARGOS LT has been shown to be greater than the Lenstar's LT by 0.22 mm [4] and the OA-2000 central corneal thickness (CCT) has been shown to be 30 μm less than the IOLMaster 700's CCT [17].

Key points of the history section

- Haigis calibrated optical biometry to immersion segmental ultrasound biometry.
- He used sum-of-segments AL for ultrasound, but couldn't for optical biometry because optical LT was not available.
- Sum-of-segments AL can be well-approximated by using only LT and AL (CMAL formula). Note, this has currently only been shown on the Lenstar biometer.
- "Single Refractive Index" and "composite" are technically incorrect terms for traditional AL.
- It is not yet finalized as to which formulas sum-of-segments AL makes better or worse. Simple vergence formulas have been shown to be better at the extremes when sum-of-segments AL is used instead of traditional AL. Newer formulas, designed with only optical biometry, seem to adjust to optical AL, and in fact, may be made worse with sum-of-segments AL.
- It is comparably easy to empirically standardize traditional AL across biometers because it only requires that the corneal and retinal interfaces (RPE) are measured. It is complex to standardize sum-of-segments AL because it requires consistent industry-wide agreement for:
  - Group RI values for the four eye segments.
  - A scaling formula because biometers measuring wavelengths range from 780 to 1300 nm.
  - The definition of segment interface locations (where on a spike to place the cursor).

Segments

There is a general uniformity of axial length measurements [10]. Each biometer tends to give the

same traditional axial length (AL). For there to be uniformity of sum-of-segments AL between biometers, however, there needs to be uniformity of the segment lengths. This has not been the case so far. Segment lengths are not as standardized as traditional AL. This could create a scenario where IOL power formulas need to vary based on measuring device, which is not ideal.

This section will evaluate the magnitude of the differences in segment lengths as well as why these differences exist. Some generalizations about measured ocular segments will be presented.

The geometric lengths of segments are calculated according to Eq. (11.3). A machine measures the optical path length (OPL) in air of the segment and divides it by that segment's refractive index (RI), given the wavelength used by the machine.

Recently, 1695 eyes were measured with a Lenstar [18]; OPLs were obtained for all ocular segments. Thirteen RI models were used to find segment RIs for a measuring wavelength of 820 nm. A fourteenth RI model was added for this chapter. The calculated geometric lengths of the segments varied, depending on the model used. The article described how to standardize sum-of-segments axial length for various RI models. For this study, the vitreous OPL started at the posterior lens surface and ended at the RPE. So the vitreous actually should probably have been called the vitreo-retinal complex because it always included the retinal thickness.

Table 11.1 is modified from that article [18]. Each model gives a different unadjusted sum-of-segments axial length (sixth column in Table 11.1). This is the total sum-of-segments AL from anterior cornea to retinal pigment epithelium (RPE) using the Lenstar measurements with RI values from the RI model listed in column 1. Note the large disparity of average ALs in column 6, depending on the RI method used. The

Table 11.1 Mean segment and unadjusted sums-of segments length for the different refractive index models using 1695 eyes originally measured with Lenstar biometer. Each value represents the average for all 1695 values (mean axial length from Lenstar printout = 23.76 mm; table is modified from Cooke et al. [18])

Refractive index model	Cornea (mm)	Aqueous (mm)	Lens (mm)	Vitreous (mm)	Unadjusted sum-of-segments AL (mm)	Theoretical retinal thickness (mm)
Navarro	0.536	2.70	4.60	16.03	23.86	0.106
D&M Le Grand (589)	0.536	2.70	4.60	16.04	23.89	0.127
D&M Le Grand (555)	0.537	2.70	4.61	16.06	23.91	0.147
A&S Le Grand (589)	0.537	2.70	4.61	16.06	23.91	0.153
Cornu Le Grand	0.537	2.71	4.60	16.07	23.91	0.155
A&S Le Grand (555)	0.537	2.71	4.61	16.08	23.94	0.177
D&M-Gullstrand (589)	0.537	2.70	4.67	16.04	23.96	0.198
Lenstar RIs	0.553	2.70	4.64	16.07	23.96	0.201
D&M-Gullstrand (555)	0.537	2.71	4.68	16.06	23.98	0.219
A&S Gullstrand (589)	0.537	2.71	4.67	16.06	23.98	0.224
A&S Cauchy (HL)	0.538	2.71	4.66	16.08	23.98	0.226
A&S Gullstrand (555)	0.538	2.71	4.68	16.08	24.01	0.248
A&S Cauchy (LL)	0.538	2.71	4.73	16.08	24.05	0.293
Liou & Brennan	0.546	2.75	4.77	16.33	24.40	0.636

average sum-of-segments AL for the 1695 eyes varied between 23.86 and 24.40 mm.

The last, seventh, column shows the adjustment to subtract from every AL to make the mean of that RI model equal to the mean traditional AL displayed by the Lenstar. Theoretically, if the values of an RI model were correct, the sum-of-segments AL would be the actual distance from the anterior cornea to the RPE. The Lenstar machine printout intentionally reports AL distance to the internal limiting membrane of the retina. The difference between the average Lenstar-displayed AL (23.76 mm) and the value in column 6 is listed in column 7. This is theoretically the difference between the RPE and the ILM. This would be the retinal thickness. That is why the last column is labeled "Theoretical Retinal Thickness."

The study found that "when the shortest *adjusted* sum-of-segments AL was subtracted from the longest one for each eye, mean difference was only 0.01 ± 0.01 mm and the maximum difference for any eye was only 0.04 mm." This adjustment method standardizes sum-of-segments AL well, even at extreme ALs. The Liou and Brennan unadjusted length was not included in that analysis. When adjusted, it varied only slightly more than the other methods.

Some items are notable about this table. The first is that several of the theoretical retinal thicknesses in column 7 are outside the physiological range for retina. This is particularly true for the Navarro schematic eye with a retinal thickness of only 106 μm and for the Liou and Brennan model which has a retinal thickness of 636 μm.

The sum-of-segments method is used by the ARGOS as well. The ARGOS was not included in this study, but it would have been near the bottom of the list because its theoretical retinal thickness is 300 μm.

There is one other commercial machine which measures sum-of-segments AL, the Galilei G6.

It actually displays both traditional and sum-of-segments AL. It uses the label "tAL (total axial length)" for sum-of-segments axial length. It defines this as "the distance from the anterior cornea to the posterior retina; optical axial length is converted to geometrical axial length using segment-specific, wavelength-adjusted, group refractive indices; for use with specifically designed formulas such as Okulix, etc." It is important to note that this axial length is different from all other sum-of-segments AL in that it is the *unadjusted* sum-of-segments AL, equivalent to column 6 in Table 11.1. Two cautions are in order:

1. It is the only commercially available sum-of-segments AL which is calculated to the retinal pigment epithelium. This has the potential to be the most accurate AL, but all other biometers adjust their AL to the anterior retina. Caution: Using tAL with standard formula lens constants could give wildly unexpected results.
2. Ziemer has not released the refractive index model (segmental refractive indices) used in developing tAL. So it is uncertain what theoretical retinal thickness to subtract in order to standardize the Galilei G6 AL to the standard IOL power formulas and lens constants.

It is worth noting that sum-of-segments isn't really the sum of all the segments; retinal thickness is subtracted to standardize it to the traditional AL. So the sum-of-segments AL, as used clinically, is only the sum of the cornea, aqueous, lens, and vitreous. Ideally, the retinal thickness would be included because the photoreceptors are located at the posterior retinal surface, not the anterior retinal surface.

Though the sum-of-segments AL can be standardized between machines, Table 11.1 shows that the segments can vary wildly; this is particularly true for the vitreous (because it is the longest) and for the lens (because it is the least understood). Haag-Streit and Movu are to be commended because other than for the Lenstar and ARGOS, companies don't list the segment RIs or OPLs that their biometers use.

To gain a better understanding of how the machine segments compare, several generalizations or "rules of thumb" are presented in Table 11.2. These derive from Table 11.3, which contains all the summaries for the comparative studies presented in Tables 11.4, 11.5, 11.6, 11.7,

Table 11.2 Generalizations from Tables 11.3, 11.4, 11.5, 11.6, and 11.7

Central corneal thickness	Anterior chamber depth	Lens thickness	Axial length
Lenstar ≈ IOLM 700 Pentacam ≈ US	Anterion ≈ OA-2000 OA-2000 ≈ Argos	OA-2000 ≈ Argos Argos ≈ Anterion	*All axial lengths are similar except for ARGOS, which is shorter in long eyes and longer in short eyes.*
US > (7μ) Lenstar; almost all others are smaller than Lenstar	Aladdin ≈ Lenstar Lenstar ≈ IOLM 700	Argos > (0.04 mm) IOLM 700 IOLM 700 > (0.04 mm) Lenstar	
IOLMaster 00 > (18μ) Argos *Argos > (10μ) OA-2000*	Argos > (0.06 mm) Lenstar Lenstar > (0.05 mm) IOLMaster 500	*Almost all are >LS* *Pent AXL did not measure LT*	

IOLM IOLMaster, *Pent AXL* Pentacam AXL. Pentacam axial length values were not listed in table because there were less than 300 such eyes available

Table 11.3 Summary (with weighted averages from Tables 11.4, 11.5, 11.6, 11.7, and 11.8)

Comparisons	*N*	CCT (μm)	ACD (mm)	LT (mm)	AL (mm)
Aladdin minus IOLMaster 500	422		0.08		0.02
OA-2000 minus IOLMaster 500	994		0.03		−0.01
IOLM-700 minus IOLMaster 500	742		−0.01		0.00
Lenstar minus IOLMaster 500	2696		0.05		0.02
Aladdin minus Lenstar	434	−10	0.00	0.16	0.00
Argos minus Lenstar	356	−9	0.06	0.22	−0.01
IOLM-700 minus Lenstar	1168	1	−0.01	0.04	0.01
OA-2000 minus Lenstar	377	−13	0.05	0.06	−0.02
Pent (AXL) minus Lenstar	815	4	N/A		N/A
US minus Lenstar	1432	7			
Argos minus IOLMaster 700	1143	−18	0.09	0.04	−0.05
Anterion minus IOLMaster 700	708	−5	0.07	0.07	−0.02
OA-2000 minus IOLMaster 700	793	−28	0.06	0.04	−0.02
OA-2000 minus Argos	690	−10	−0.03	0.00	0.04

US ultrasound, *IOLM* IOLMaster, *Pent (AXL)* Pentacam combined with Pentacam AXL. Sample size (*N*) is not necessarily the value for all segments in a given row (e.g., in the "ARGOS minus Lenstar" row, 356 eyes were evaluated, but only 62 eyes measured ACD)

Table 11.4 Machine CCT minus Lenstar CCT

Machine	Sample size	μm
Ultrasound [22]	80	10
Ultrasound [23]	256	3
Ultrasound [24]	55	1.2
Ultrasound [24]	50	−1.7
Ultrasound [25]	65	5.6
Ultrasound [26]	530	13.2
Ultrasound [27]	50	13
Ultrasound [28]	76	7
Ultrasound [29]	184	−3.5
Ultrasound [30]	86	8
Galilei [22]	80	28
Galilei [31]	100	17
Galilei [32]	47	15
Galilei [33]	120	−1
Pentacam [29]	184	7
Pentacam [28]	76	22
Pentacam [34]	108	5
Pentacam [35]	37	3
Pentacam [36]	27	−9
Pentacam [32]	47	6
Pentacam [33]	120	2
Sirius [37]	40	4
Sirius [23]	256	−7
Sirius [27]	50	−4
RTVue OCT [23]	256	−7
RTVue-OCT [27]	50	−4

CCT central corneal thickness

and 11.8. These were drawn from comparisons found in the literature. They are almost all English-language articles from peer-reviewed journals. This is not meant to be an exhaustive list. It is hoped that these tables will highlight the

Table 11.5 Machine minus IOLMaster 500

Machine	*N*	CCT (μm)	ACD (mm)	LT (mm)	AL (mm)
Aladdin [38]	231		0.10		0.04
Aladdin [39]	60		0.16		0.01
Aladdin [39]	56		0.05		−0.01
Aladdin [40]	75		0.00		0.01
ARGOS [41]	129		−0.06		−0.03
ARGOS [4]	42		0.17		0.01
OA-2000 [42]	119		N/A		0.00
OA-2000 [43]	65		0.01		0.01
OA-2000 [44]	58		0.01		0.11
OA-2000 [45]	108		0.01		−0.06
OA-2000 [46]	138		0.18		−0.05
OA-2000 [47]	102		−0.09		−0.06
OA-2000 [42]	119		N/A		0.00
OA-2000 [48]	140		0.05		0.00
OA-2000 [49]	99		−0.01		−0.01
OA-2000 [50]	46		−0.06		0.02
IOLM700 [41]	129		−0.07		0.00
IOLM700 [42]	119		N/A		0.00
IOLM700 [51]	111		0.02		0.00
IOLM700 [52]	171		−0.08		−0.01
IOLM700 [53]	100		0.04		0.02
IOLM700 [54]	112		0.11		0.00
Lenstar [54]	112		0.12		0.01
Lenstar [55]	51		0.06		0.01
Lenstar [4]	42		0.24		0.02
Lenstar [38]	231		0.10		0.04
Lenstar [56]	112		0.10		0.01
Lenstar [57]	100		0.14		0.02
Lenstar [58]	105		0.10		0.02
Lenstar [46]	138		0.01		0.02
Lenstar [59]	200		0.17		0.01
Lenstar [60]	76		0.05		0.03
Lenstar [61]	125		0.02		0.00
Lenstar [62]	109		N/A		0.01
Lenstar [63]	76		N/A		0.01
Lenstar [64]	1079		0.01[a]		0.00
Lenstar [48]	140		0.00		0.03

N sample size, *CCT* central corneal thickness, *ACD* anterior chamber depth, *LT* lens thickness, *AL* axial length

[a] ACD is unpublished data obtained from Cooke and Cooke [64]

wide variation present in measuring segments and to provide some of the supporting data for the generalizations presented in Table 11.2. The most-notable findings were italicized. Any such generalizations are likely to change as more studies become available.

Table 11.6 Machine minus Lenstar

Machine	*N*	CCT (μm)	ACD (mm)	LT (mm)	AL (mm)
Aladdin [38]	231	N/A	0.00	N/A	0.00
Aladdin [65]	101	−10	−0.01	0.16	−0.01
Aladdin [66]	102	N/A	0.00	N/A	0.01
ARGOS [4]	62	N/A	−0.07	0.22	−0.01
ARGOS [67]	294	−9	0.09	N/A	−0.01
IOLM700 [68]	64	N/A	−0.02	0.14	0.00
IOLM700 [69]	183	−5	0.03	−0.03	0.01
IOLM700 [70]	129	−1	−0.02	−0.03	0.00
IOLM700 [71]	127	−2	0.01	−0.02	0.13
IOLM700 [72]	80	3	−0.02	0.04	0.00
IOLM700 [73]	100	6	−0.03	0.06	−0.01
IOLM700 [74]	48	6	N/A	0.04	N/A
IOLM700 [74]	50	5	N/A	0.08	N/A
IOLM700 [75]	164	5	−0.07	0.17	−0.01
IOLM700 [54]	112	N/A	−0.01	N/A	−0.01
IOLM700 [51]	111	0	N/A	0.02	0.00
OA-2000 [46]	138	N/A	0.08	N/A	−0.03
OA-2000 [76]	99	−13	0.00	0.08	0.01
OA-2000 [48]	140	N/A	0.06	0.04	−0.03
Pent-AXL [77]	136	−10	0.00	N/A[a]	−0.02
Pent-AXL [78]	40	4	0.03	N/A[a]	−0.08
Pent-AXL [78]	40	6	−0.04	N/A[a]	0.02

N sample size, *CCT* central corneal thickness, *ACD* anterior chamber depth, *LT* lens thickness, *AL* axial length

[a] Currently, the Pentacam AXL or "AXL Wave" has a PCI system like the IOL Master 500. As such it does not include a lens thickness

Table 11.7 Machine minus IOLMaster 700

Machine	*N*	CCT (μm)	ACD (mm)	LT (mm)	AL (mm)
ARGOS [41]	129	−24	0.00	0.07	−0.03
ARGOS [79]	106	−26	0.10	0.01	−0.08
ARGOS [42]	119	N/A	N/A	N/A	0.00
ARGOS [80]	218	−5	0.12	0.08	−0.01
ARGOS [17]	571	−20	0.10	0.03	−0.07
Anterion [81]	389	−6	0.07	0.06	−0.01
Anterion [82]	49	−7	0.06	−0.06	0.00
Anterion [71]	127	2	0.04	0.07	−0.08
Anterion [83]	41	1	0.08	0.09	0.01
Anterion [84]	102	−7	0.07	0.06	–
Anterion [85]	125	−9	0.07	0.07	−0.01
Anterion [86]	78	–	0.07	0.07	−0.01
OA-2000 [42]	119	N/A	N/A	N/A	−0.01
OA-2000 [17]	571	−30	0.07	0.03	−0.02
OA-2000 [87]	103	−17	0.00	0.08	0.00

N sample size, *CCT* central corneal thickness, *ACD* anterior chamber depth, *LT* lens thickness, *AL* axial length

Table 11.8 Machine minus ARGOS

Machine	*N*	CCT (μm)	ACD (mm)	LT (mm)	AL (mm)
OA-2000 [42]	119	N/A	N/A	N/A	0.00
OA-2000 [17]	571	−10	−0.03	0.00	0.05

N sample size, *CCT* central corneal thickness, *ACD* anterior chamber depth, *LT* lens thickness, *AL* axial length

Comparative studies were included in Tables 11.3, 11.4, 11.5, 11.6, and 11.7 only if there were at least two papers making the same analysis. In addition, at least 300 eyes total were required. Instead of showing the absolute differences between machines, the values in Tables 11.3, 11.4, 11.5, 11.6, and 11.7 show the direction of the difference. This should identify if one machine consistently measures shorter or longer than another. Hopefully, adjustments can be made to equalize segment distances.

Summary of Segments

- Other than for the Argos biometer, AL between biometers is similar. Machines have been calibrated to the original IOLMaster.
- Argos has been adjusted so that normal ALs are fairly similar to the original IOLMaster.
- Galilei G6 has two AL options. One of them has been calibrated to the IOLMaster; the other (tAL) has not been calibrated to the IOLMaster and might give markedly different predictions in "unsuspecting" IOL power formulas.
- Segmental thicknesses, especially LTs, differ between biometers. This means that the CMAL formula might only work on the Lenstar machine.
- Though the AL can be made to be equivalent to the sum-of-segments AL of other machines, segments are likely to vary wildly. This is particularly true of the vitreous (because it is the longest) and the lens (because it is the least understood).
- Other than for the Lenstar and ARGOS, companies don't list either the RIs or the OPLs their biometers use. Haag-Streit and MOVU are to be commended.
- Sum-of-segments AL appears to help original vergence formulas, assuming that it is adjusted to original IOLMaster AL by subtracting a theoretical retinal thickness.

Areas for Potential Improvement

Some questions remain, such as, "Why does the AL measurement decrease after cataract extraction?" Many studies have shown the AL measures about 0.07 mm shorter after cataract extraction. There seem to be three possible answers: (1) RIs are incorrect; (2) segmental AL is needed, instead of traditional AL; or (3) the eye

shortens after cataract extraction. The answer is currently unknown.

If ALs were all correct, then merely adding 200 μm to the adjusted sum-of-segments AL would give the distance to the RPE. But we don't know that all measurements (traditional AL and all of the ocular segments) are correct. Hopefully, work will be done to try to determine the physiological RIs for the various measuring wavelengths used.

Ueda [19], Prinz [20], and Cooke [21] have shown that increasing cataract density causes eyes to measure longer. Presumably, this is due to the lenticular RI increasing more than the machine predicts, thereby measuring the eye as too long. Could biometers auto-adjust RIs based on the density of the cataract?

Probably, the biggest future improvement would be for companies to publicize their OPLs. If not, they could publicize their RIs; OPLs could be back-calculated from Eq. (11.3). To date, only Haag-Streit (Lenstar) and Movu (ARGOS) have released their RIs.

Chapter Summary

- The traditional ALs we measure may not be physiologically accurate.
  - Optical biometry approximately equals immersion US AL, and immersion US AL might not be physiologically correct, particularly since the standard sound velocities have not been challenged in decades.
  - Current techniques tend to make displayed ALs equivalent between machines.
- Sum-of-segments ALs are different from traditional AL, especially at extremes.
  - Traditional AL reports measurements to the ILM, optical sum-of-segments AL measures to the RPE; they can be made similar by subtracting retinal thickness from each sum-of-segments AL.
  - RIs are not currently known.
  - Different sum-of-segments ALs can be made equivalent to each other in their means, even with widely varied RIs. This can limit differences between RI models.
  - Individual segment lengths of the eye (e.g., the lens) can vary widely, with varied RIs. There is not currently an acceptable standard for these thicknesses, but knowing the OPLs for the segments would enable others to help standardize segment lengths.
  - Unadjusted optical sum-of-segments AL, measuring to the RPE, likely more closely approximates physiologically correct (accurate) values if accurate RIs can be obtained.
- Creating AL measurements with improved physiologic accuracy holds promise for further improvement of IOL power calculations.

Acknowledgment Special thanks to Marwan Suheimat for the explanation of coherence and to Michael Trost of Zeiss for the translation of Haigis's German article as well as extensive proof-reading of this chapter.

References

1. Shammas HJ, Shammas MC, Jivrajka RV, Cooke DL, Potvin R. Effects on IOL power calculation and expected clinical outcomes of axial length measurements based on multiple vs single refractive indices. Clin Ophthalmol. 2020;14:1511–9. https://doi.org/10.2147/OPTH.S256851.
2. Goto S, Maeda N, Noda T, Ohnuma K, Koh S, Iehisa I, Nishida K. Comparison of composite and segmental methods for acquiring optical axial length with swept-source optical coherence tomography. Sci Rep. 2020;10(1):4474. https://doi.org/10.1038/s41598-020-61391-7.
3. Wang L, Cao D, Weikert MP, Koch DD. Calculation of axial length using a single group refractive index versus using different refractive indices for each ocular segment: theoretical study and refractive outcomes. Ophthalmology. 2019;126(5):663–70. https://doi.org/10.1016/j.ophtha.2018.12.046. Epub 2018 Dec 31.
4. Shammas HJ, Ortiz S, Shammas MC, Kim SH, Chong C. Biometry measurements using a new large-coherence-length swept-source optical coherence tomographer. J Cataract Refract Surg. 2016;42(1):50–61. https://doi.org/10.1016/j.jcrs.2015.07.042.
5. Vogel A, Dick HB, Krummenauer F. Reproducibility of optical biometry using partial coherence interferometry: intraobserver and interobserver reliability. J Cataract Refract Surg. 2001;27(12):1961–8. https://doi.org/10.1016/s0886-3350(01)01214-7.

6. Chong C, Suzuki T, Morosawa A, Sakai T. Spectral narrowing effect by quasi-phase continuous tuning in high-speed wavelength-swept light source. Opt Express. 2008;16(25):21105–18. https://doi.org/10.1364/oe.16.021105.
7. Haigis W, Lege B, Miller N, Schneider B. Comparison of immersion ultrasound biometry and partial coherence interferometry for intraocular lens calculation according to Haigis. Graefes Arch Clin Exp Ophthalmol. 2000;238(9):765–73. https://doi.org/10.1007/s004170000188.
8. Haigis W, Kohnen T, editors. Modern cataract surgery, Dev ophthalmol, vol. 34. Basel: Karger; 2002. p. 119–30. https://doi.org/10.1159/000060791.
9. Haigis W , Mlynski J. Comparative axial length measurements using optical and acoustic biometry in normal persons and in patients with retinal lesions. In: White Paper, Carl Zeiss Meditec. 2009.
10. Optische und geometrische Weglänge in der Laserinterferenzbiometrie. http://www.dgii.org/uploads/jahresband/2013/025_Haigis.pdf. Accessed 14 Jan 2021.
11. Preussner PR, Olsen T, Hoffmann P, Findl O. Intraocular lens calculation accuracy limits in normal eyes. J Cataract Refract Surg. 2008;34(5):802–8. https://doi.org/10.1016/j.jcrs.2008.01.015.
12. Olsen T. Calculation of intraocular lens power: a review. Acta Ophthalmol Scand. 2007;85(5):472–85. https://doi.org/10.1111/j.1600-0420.2007.00879.x. Epub 2007 Apr 2.
13. Fam HB, Lim KL. Improving refractive outcomes at extreme axial lengths with the IOLMaster: the optical axial length and keratometric transformation. Br J Ophthalmol. 2009;93(5):678–83. https://doi.org/10.1136/bjo.2008.148452. Epub 2009 Jan 23.
14. Wang L, Shirayama M, Ma XJ, Kohnen T, Koch DD. Optimizing intraocular lens power calculations in eyes with axial lengths above 25.0 mm. J Cataract Refract Surg. 2011;37(11):2018–27. https://doi.org/10.1016/j.jcrs.2011.05.042.
15. U.S. Food and Drug Administration. 510(K) summary. Available at: https://www.accessdata.fda.gov/cdrh_docs/pdf8/K082891.pdf. Accessed 14 Jan 2021.
16. Cooke DL, Cooke TL. A comparison of two methods to calculate axial length. J Cataract Refract Surg. 2019;45(3):284–92. https://doi.org/10.1016/j.jcrs.2018.10.039.
17. Tamaoki A, Kojima T, Hasegawa A, Yamamoto M, Kaga T, Tanaka K, Ichikawa K. Clinical evaluation of a new swept-source optical coherence biometer that uses individual refractive indices to measure axial length in cataract patients. Ophthalmic Res. 2019;62(1):11–23. https://doi.org/10.1159/000496690. Epub 2019 Mar 19.
18. Cooke DL, Cooke TL, Suheimat M, Atchison DA. Standardizing sum-of-segments axial length using refractive index models. Biomed Opt Express. 2020;11(10):5860–70. https://doi.org/10.1364/BOE.400471.
19. Ueda T, Ikeda H, Ota T, Matsuura T, Hara Y. Relationship between postoperative refractive outcomes and cataract density: multiple regression analysis. J Cataract Refract Surg. 2010;36(5):806–9. https://doi.org/10.1016/j.jcrs.2009.12.024.
20. Prinz A, Neumayer T, Buehl W, Kiss B, Sacu S, Drexler W, Findl O. Influence of severity of nuclear cataract on optical biometry. J Cataract Refract Surg. 2006;32(7):1161–5. https://doi.org/10.1016/j.jcrs.2006.01.101.
21. Cooke DL, Cooke TL, Atchison DA. Effect of cataract-induced refractive change on intraocular lens power formula predictions. Biomed Opt Express. 2021;12(5):2550–6. https://doi.org/10.1364/BOE.422190.
22. Can E, Eser-Ozturk H, Duran M, Cetinkaya T, Arıturk N. Comparison of central corneal thickness measurements using different imaging devices and ultrasound pachymetry. Indian J Ophthalmol. 2019;67(4):496–9. https://doi.org/10.4103/ijo.IJO_960_18.
23. Şimşek A, Bilak Ş, Güler M, Çapkin M, Bilgin B, Reyhan AH. Comparison of central corneal thickness measurements obtained by rtvue oct, lenstar, sirius topography, and ultrasound pachymetry in healthy subjects. Semin Ophthalmol. 2016;31(5):467–72. https://doi.org/10.3109/08820538.2014.962173. Epub 2014 Nov 20.
24. Huang J, Liao N, Savini G, Li Y, Bao F, Yu Y, Yu A, Wang Q. Measurement of central corneal thickness with optical low-coherence reflectometry and ultrasound pachymetry in normal and post-femtosecond laser in situ keratomileusis eyes. Cornea. 2015;34(2):204–8. https://doi.org/10.1097/ICO.0000000000000329.
25. Koktekir BE, Gedik S, Bakbak B. Comparison of central corneal thickness measurements with optical low-coherence reflectometry and ultrasound pachymetry and reproducibility of both devices. Cornea. 2012;31(11):1278–81. https://doi.org/10.1097/ICO.0b013e31823f7701.
26. Gursoy H, Sahin A, Basmak H, et al. Lenstar versus ultrasound for ocular biometry in a pediatric population. Optom Vis Sci. 2011;88:912–9.
27. Bayhan HA, Aslan Bayhan S, Can I. Comparison of central corneal thickness measurements with three new optical devices and a standard ultrasonic pachymeter. Int J Ophthalmol. 2014;7(2):302–8. https://doi.org/10.3980/j.issn.2222-3959.2014.02.19.
28. Borrego-Sanz L, Sáenz-Francés F, Bermudez-Vallecilla M, Morales-Fernández L, Martínez-de-la-Casa JM, Santos-Bueso E, Jañez L, García-Feijoo J. Agreement between central corneal thickness measured using Pentacam, ultrasound pachymetry, specular microscopy and optic biometer Lenstar LS 900 and the influence of intraocular pressure. Ophthalmologica. 2014;231(4):226–35. https://doi.org/10.1159/000356724. Epub 2014 Mar 13.
29. Tai LY, Khaw KW, Ng CM, Subrayan V. Central corneal thickness measurements with differ-

ent imaging devices and ultrasound pachymetry. Cornea. 2013;32(6):766–71. https://doi.org/10.1097/ICO.0b013e318269938d.
30. El Chehab H, Giraud JM, Le Corre A, Chave N, Durand F, Kuter S, Ract-Madoux G, Swalduz B, Mourgues G, Dot C. Comparaison de la biométrie sans contact cornéen par LENSTAR LS 900 et de la biométrie contact par OCUSCAN RXP dans le cadre de la délégation de tâches [Comparison between Lenstar LS 900 non-contact biometry and OcuScan RXP contact biometry for task delegation]. J Fr Ophtalmol. 2011;34(3):175–80. French. https://doi.org/10.1016/j.jfo.2010.09.026. Epub 2011 Jan 22.
31. Huerva V, Ascaso FJ, Soldevila J, Lavilla L. Comparison of anterior segment measurements with optical low-coherence reflectometry and rotating dual Scheimpflug analysis. J Cataract Refract Surg. 2014;40(7):1170–6. https://doi.org/10.1016/j.jcrs.2013.10.045. Epub 2014 May 20.
32. Han SH, Hwang HS, Shin MC, Han KE. Comparison of central corneal thickness and anterior chamber depth measured using three different devices. J Korean Ophthalmol Soc. 2015;56:694–701.
33. Miranda I. Comparación de los valores del espesor corneal central según los equipos Lenstar, Galilei y Pentacam. Rev Cubana Oftalmol. 2012;25(1):65–71.
34. Huang J, Pesudovs K, Wen D, Chen S, Wright T, Wang X, Li Y, Wang Q. Comparison of anterior segment measurements with rotating Scheimpflug photography and partial coherence reflectometry. J Cataract Refract Surg. 2011;37(2):341–8. https://doi.org/10.1016/j.jcrs.2010.08.044.
35. Sen E, Inanc M, Elgin U, Yilmazbas P. Comparison of anterior segment measurements with LenStar and Pentacam in patients with newly diagnosed glaucoma. Int Ophthalmol. 2018;38(1):171–4. https://doi.org/10.1007/s10792-016-0440-z. Epub 2017 Jan 21.
36. O'Donnell C, Hartwig A, Radhakrishnan H. Comparison of central corneal thickness and anterior chamber depth measured using LenStar LS900, Pentacam, and Visante AS-OCT. Cornea. 2012;31(9):983–8. https://doi.org/10.1097/ICO.0b013e31823f8e2f.
37. Chen W, McAlinden C, Pesudovs K, Wang Q, Lu F, Feng Y, Chen J, Huang J. Scheimpflug-Placido topographer and optical low-coherence reflectometry biometer: repeatability and agreement. J Cataract Refract Surg. 2012;38(9):1626–32. https://doi.org/10.1016/j.jcrs.2012.04.031. Epub 2012 Jul 3.
38. Ortiz A, Galvis V, Tello A, Viaña V, Corrales MI, Ochoa M, Rodriguez CJ. Comparison of three optical biometers: IOLMaster 500, Lenstar LS 900 and Aladdin. Int Ophthalmol. 2019;39(8):1809–18. https://doi.org/10.1007/s10792-018-1006-z. Epub 2018 Aug 22.
39. Hoffer KJ, Shammas HJ, Savini G, Huang J. Multicenter study of optical low-coherence interferometry and partial-coherence interferometry optical biometers with patients from the United States and China. J Cataract Refract Surg. 2016;42(1):62–7. https://doi.org/10.1016/j.jcrs.2015.07.041.
40. Mandal P, Berrow EJ, Naroo SA, Wolffsohn JS, Uthoff D, Holland D, Shah S. Validity and repeatability of the Aladdin ocular biometer. Br J Ophthalmol. 2014;98(2):256–8. https://doi.org/10.1136/bjophthalmol-2013-304002. Epub 2013 Nov 13. Erratum in: Br J Ophthalmol. 2015 Dec;99(12):1746.
41. Yang CM, Lim DH, Kim HJ, Chung TY. Comparison of two swept-source optical coherence tomography biometers and a partial coherence interferometer. PLoS One. 2019;14(10):e0223114. https://doi.org/10.1371/journal.pone.0223114.
42. Huang J, Chen H, Li Y, Chen Z, Gao R, Yu J, Zhao Y, Lu W, McAlinden C, Wang Q. Comprehensive comparison of axial length measurement with three swept-source OCT-based biometers and partial coherence interferometry. J Refract Surg. 2019;35(2):115–20. https://doi.org/10.3928/1081597X-20190109-01.
43. Huang J, Savini G, Hoffer KJ, Chen H, Lu W, Hu Q, Bao F, Wang Q. Repeatability and interobserver reproducibility of a new optical biometer based on swept-source optical coherence tomography and comparison with IOLMaster. Br J Ophthalmol. 2017;101(4):493–8. https://doi.org/10.1136/bjophthalmol-2016-308352. Epub 2016 Aug 8.
44. Ghaffari R, Mahmoudzadeh R, Mohammadi SS, Salabati M, Latifi G, Ghassemi H. Assessing the validity of measurements of swept-source and partial coherence interferometry devices in cataract patients. Optom Vis Sci. 2019;96(10):745–50. https://doi.org/10.1097/OPX.0000000000001433.
45. Hua Y, Qiu W, Xiao Q, Wu Q. Precision (repeatability and reproducibility) of ocular parameters obtained by the Tomey OA-2000 biometer compared to the IOLMaster in healthy eyes. PLoS One. 2018;13(2):e0193023. https://doi.org/10.1371/journal.pone.0193023.
46. Goebels S, Pattmöller M, Eppig T, Cayless A, Seitz B, Langenbucher A. Comparison of 3 biometry devices in cataract patients. J Cataract Refract Surg. 2015;41(11):2387–93. https://doi.org/10.1016/j.jcrs.2015.05.028.
47. Kongsap P. Comparison of a new optical biometer and a standard biometer in cataract patients. Eye Vis (Lond). 2016;3:27. https://doi.org/10.1186/s40662-016-0059-1.
48. Reitblat O, Levy A, Kleinmann G, Assia EI. Accuracy of intraocular lens power calculation using three optical biometry measurement devices: the OA-2000, Lenstar-LS900 and IOLMaster-500. Eye (Lond). 2018;32(7):1244–52. https://doi.org/10.1038/s41433-018-0063-x. Epub 2018 Mar 12.
49. Guo XX, You R, Li SS, Yang XF, Zhao L, Zhang F, Wang YL, Chen X. Comparison of ocular parameters of two biometric measurement devices in highly myopic eyes. Int J Ophthalmol. 2019;12(10):1548–54. https://doi.org/10.18240/ijo.2019.10.05.
50. Du YL, Wang G, Huang HC, Lin LY, Jin C, Liu LF, Liu XR, Zhang MZ. Comparison of OA-2000 and

IOL Master 500 using in cataract patients with high myopia. Int J Ophthalmol. 2019;12(5):844–7. https://doi.org/10.18240/ijo.2019.05.23.
51. Kunert KS, Peter M, Blum M, Haigis W, Sekundo W, Schütze J, Büehren T. Repeatability and agreement in optical biometry of a new swept-source optical coherence tomography-based biometer versus partial coherence interferometry and optical low-coherence reflectometry. J Cataract Refract Surg. 2016;42(1):76–83. https://doi.org/10.1016/j.jcrs.2015.07.039.
52. Akman A, Asena L, Güngör SG. Evaluation and comparison of the new swept source OCT-based IOLMaster 700 with the IOLMaster 500. Br J Ophthalmol. 2016;100(9):1201–5. https://doi.org/10.1136/bjophthalmol-2015-307779. Epub 2015 Dec 16.
53. Srivannaboon S, Chirapapaisan C, Chonpimai P, Loket S. Clinical comparison of a new swept-source optical coherence tomography-based optical biometer and a time-domain optical coherence tomography-based optical biometer. J Cataract Refract Surg. 2015;41(10):2224–32. https://doi.org/10.1016/j.jcrs.2015.03.019.
54. Song JS, Yoon DY, Hyon JY, Jeon HS. Comparison of ocular biometry and refractive outcomes using IOL Master 500, IOL Master 700, and Lenstar LS900. Korean J Ophthalmol. 2020;34(2):126–32. https://doi.org/10.3341/kjo.2019.0102.
55. Mylonas G, Sacu S, Buehl W, Ritter M, Georgopoulos M, Schmidt-Erfurth U. Performance of three biometry devices in patients with different grades of age-related cataract. Acta Ophthalmol. 2011;89(3):e237–41. https://doi.org/10.1111/j.1755-3768.2010.02042.x. Epub 2011 Feb 11.
56. Buckhurst PJ, Wolffsohn JS, Shah S, Naroo SA, Davies LN, Berrow EJ. A new optical low coherence reflectometry device for ocular biometry in cataract patients. Br J Ophthalmol. 2009;93(7):949–53. https://doi.org/10.1136/bjo.2008.156554. Epub 2009 Apr 19.
57. Hoffer KJ, Shammas HJ, Savini G. Comparison of 2 laser instruments for measuring axial length. J Cataract Refract Surg. 2010;36(4):644–8. https://doi.org/10.1016/j.jcrs.2009.11.007. Erratum in: J Cataract Refract Surg. 2010 Jun;36(6):1066.
58. Epitropoulos A. Axial length measurement acquisition rates of two optical biometers in cataractous eyes. Clin Ophthalmol. 2014;8:1369–76. https://doi.org/10.2147/OPTH.S62653.
59. Holzer MP, Mamusa M, Auffarth GU. Accuracy of a new partial coherence interferometry analyser for biometric measurements. Br J Ophthalmol. 2009;93(6):807–10. https://doi.org/10.1136/bjo.2008.152736. Epub 2009 Mar 15.
60. Cruysberg LP, Doors M, Verbakel F, Berendschot TT, De Brabander J, Nuijts RM. Evaluation of the Lenstar LS 900 non-contact biometer. Br J Ophthalmol. 2010;94(1):106–10. https://doi.org/10.1136/bjo.2009.161729. Epub 2009 Aug 18.
61. Rohrer K, Frueh BE, Wälti R, Clemetson IA, Tappeiner C, Goldblum D. Comparison and evaluation of ocular biometry using a new noncontact optical low-coherence reflectometer. Ophthalmology. 2009;116(11):2087–92. https://doi.org/10.1016/j.ophtha.2009.04.019. Epub 2009 Sep 10.
62. Chen YA, Hirnschall N, Findl O. Evaluation of 2 new optical biometry devices and comparison with the current gold standard biometer. J Cataract Refract Surg. 2011;37(3):513–7. https://doi.org/10.1016/j.jcrs.2010.10.041. Epub 2011 Jan 17.
63. Jasvinder S, Khang TF, Sarinder KK, Loo VP, Subrayan V. Agreement analysis of LENSTAR with other techniques of biometry. Eye (Lond). 2011;25(6):717–24. https://doi.org/10.1038/eye.2011.28. Epub 2011 Mar 11.
64. Cooke DL, Cooke TL. Comparison of 9 intraocular lens power calculation formulas. J Cataract Refract Surg. 2016;42(8):1157–64. https://doi.org/10.1016/j.jcrs.2016.06.029.
65. Yeu E. Agreement of ocular biometry measurements between 2 biometers. J Cataract Refract Surg. 2019;45(8):1130–4. https://doi.org/10.1016/j.jcrs.2019.03.016. Epub 2019 Jul 3.
66. McAlinden C, Gao R, Yu A, Wang X, Yang J, Yu Y, Chen H, Wang Q, Huang J. Repeatability and agreement of ocular biometry measurements: Aladdin versus Lenstar. Br J Ophthalmol. 2017;101(9):1223–9. https://doi.org/10.1136/bjophthalmol-2016-309365. Epub 2017 Jan 27.
67. Cummings AB, Naughton S, Coen AM, Brennan E, Kelly GE. Comparative analysis of swept-source optical coherence tomography and partial coherence interferometry biometers in the prediction of cataract surgery refractive outcomes. Clin Ophthalmol. 2020;14:4209–20. https://doi.org/10.2147/OPTH.S278589.
68. Passi SF, Thompson AC, Gupta PK. Comparison of agreement and efficiency of a swept source-optical coherence tomography device and an optical low-coherence reflectometry device for biometry measurements during cataract evaluation. Clin Ophthalmol. 2018;12:2245–51. https://doi.org/10.2147/OPTH.S182898.
69. Hoffer KJ, Hoffmann PC, Savini G. Comparison of a new optical biometer using swept-source optical coherence tomography and a biometer using optical low-coherence reflectometry. J Cataract Refract Surg. 2016;42(8):1165–72. https://doi.org/10.1016/j.jcrs.2016.07.013.
70. El Chehab H, Agard E, Dot C. Comparison of two biometers: a swept-source optical coherence tomography and an optical low-coherence reflectometry biometer. Eur J Ophthalmol. 2019;29(5):547–54. https://doi.org/10.1177/1120672118802918. Epub 2018 Oct 7.
71. Shetty N, Kaweri L, Koshy A, Shetty R, Nuijts RMMA, Roy AS. Repeatability of biometry measured by IOLMaster 700, Lenstar LS 900 and Anterion,

and its impact on predicted intraocular lens power. J Cataract Refract Surg. 2020;47:585. https://doi.org/10.1097/j.jcrs.0000000000000494. Epub ahead of print.
72. Arriola-Villalobos P, Almendral-Gómez J, Garzón N, Ruiz-Medrano J, Fernández-Pérez C, Martínez-de-la-Casa JM, Díaz-Valle D. Agreement and clinical comparison between a new swept-source optical coherence tomography-based optical biometer and an optical low-coherence reflectometry biometer. Eye (Lond). 2017;31(3):437–42. https://doi.org/10.1038/eye.2016.241. Epub 2016 Nov 11.
73. Kurian M, Negalur N, Das S, Puttaiah NK, Haria D, Tejal SJ, Thakkar MM. Biometry with a new swept-source optical coherence tomography biometer: repeatability and agreement with an optical low-coherence reflectometry device. J Cataract Refract Surg. 2016;42(4):577–81. https://doi.org/10.1016/j.jcrs.2016.01.038.
74. Bullimore MA, Slade S, Yoo P, Otani T. An evaluation of the IOLMaster 700. Eye Contact Lens. 2019;45(2):117–23. https://doi.org/10.1097/ICL.0000000000000552.
75. Cheng H, Li J, Cheng B, Wu M. Refractive predictability using two optical biometers and refraction types for intraocular lens power calculation in cataract surgery. Int Ophthalmol. 2020;40(7):1849–56. https://doi.org/10.1007/s10792-020-01355-y. Epub 2020 Apr 15.
76. Gao R, Chen H, Savini G, Miao Y, Wang X, Yang J, Zhao W, Wang Q, Huang J. Comparison of ocular biometric measurements between a new swept-source optical coherence tomography and a common optical low coherence reflectometry. Sci Rep. 2017;7(1):2484. https://doi.org/10.1038/s41598-017-02463-z.
77. Pereira JMM, Neves A, Alfaiate P, Santos M, Aragão H, Sousa JC. Lenstar® LS 900 vs Pentacam®-AXL: comparative study of ocular biometric measurements and intraocular lens power calculation. Eur J Ophthalmol. 2018;28(6):645–51. https://doi.org/10.1177/1120672118771844. Epub 2018 May 22.
78. Ruiz-Mesa R, Abengózar-Vela A, Ruiz-Santos M. Comparison of a new Scheimpflug imaging combined with partial coherence interferometry biometer and a low-coherence reflectometry biometer. J Cataract Refract Surg. 2017;43(11):1406–12. https://doi.org/10.1016/j.jcrs.2017.08.016.
79. Omoto MK, Torii H, Masui S, Ayaki M, Tsubota K, Negishi K. Ocular biometry and refractive outcomes using two swept-source optical coherence tomography-based biometers with segmental or equivalent refractive indices. Sci Rep. 2019;9(1):6557. https://doi.org/10.1038/s41598-019-42968-3. Erratum in: Sci Rep. 2020 Jul 31;10(1):13181.
80. Sabatino F, Matarazzo F, Findl O, Maurino V. Comparative analysis of 2 swept-source optical coherence tomography biometers. J Cataract Refract Surg. 2019;45(8):1124–9. https://doi.org/10.1016/j.jcrs.2019.03.020. Epub 2019 Jun 4.
81. Fișuș AD, Hirnschall ND, Findl O. Comparison of two swept-source optical coherence tomography-based biometry devices. J Cataract Refract Surg. 2021;47(1):87–92. https://doi.org/10.1097/j.jcrs.0000000000000373.
82. Tañá-Rivero P, Aguilar-Córcoles S, Tello-Elordi C, Pastor-Pascual F, Montés-Micó R. Agreement between two swept-source OCT biometers and a Scheimpflug partial coherence interferometer. J Cataract Refract Surg. 2020;47:488. https://doi.org/10.1097/j.jcrs.0000000000000483. Epub ahead of print.
83. Oh R, Oh JY, Choi HJ, Kim MK, Yoon CH. Comparison of ocular biometric measurements in patients with cataract using three swept-source optical coherence tomography devices. BMC Ophthalmol. 2021;21(1):62. https://doi.org/10.1186/s12886-021-01826-5.
84. Tañá-Sanz P, Ruiz-Santos M, Rodríguez-Carrillo MD, Aguilar-Córcoles S, Montés-Micó R, Tañá-Rivero P. Agreement between intraoperative anterior segment spectral-domain OCT and 2 swept-source OCT biometers. Expert Rev Med Devices. 2021;18(4):387–93. https://doi.org/10.1080/17434440.2021.1905518. Epub 2021 Mar 30.
85. Panthier C, Rouger H, Gozlan Y, Moran S, Gatinel D. Comparative analysis of 2 biometers using swept-source optical coherence tomography technology. J Cataract Refract Surg. 2021;48:26. https://doi.org/10.1097/j.jcrs.0000000000000704. Epub ahead of print.
86. Pfaeffli OA, Weber A, Hoffer KJ, Savini G, Baenninger PB, Thiel MA, Taroni L, Müller L. Agreement of IOL power calculation between IOLMaster 700 and Anterion swept source optical coherence tomography-based biometers. J Cataract Refract Surg. 2021;48:535. https://doi.org/10.1097/j.jcrs.0000000000000788. Epub ahead of print.
87. Liao X, Peng Y, Liu B, Tan QQ, Lan CJ. Agreement of ocular biometric measurements in young healthy eyes between IOLMaster 700 and OA-2000. Sci Rep. 2020;10(1):3134. https://doi.org/10.1038/s41598-020-59919-y.